Received: xxx **Accepted:** xxx **Published:** xxx.
DOI. xxxxxxx
Volume xxx, Issue xxx, p.p. 1-27: xxx
Research Article

Open Access

Control and Optimization in Applied Mathematics - COAM

Solving Variable-Order Fractional Integro-Differential Equations Using the Two-Dimensional Fractional-Order Fibonacci Wavelets Operational Matrix

Shiva Karimi **Elyas Shivanian** ✉ **Zahra Barikbin**

Department of Applied Mathematics, Imam Khomeini International University, Qazvin, 34149-16818, Iran.

✉ **Correspondence:**
Elyas Shivanian
E-mail:
shivanian@sci.ikiu.ac.ir

Abstract. This paper presents a novel numerical method for solving variable-order fractional integro-differential equations using two-dimensional fractional-order Fibonacci wavelets. The proposed approach employs fractional-order Fibonacci wavelets together with their associated integral and derivative operational matrices. First, new integral and derivative operational matrices are derived. These matrices, which exhibit improved accuracy in the numerical examples reported herein, are then employed to transform the governing equation into a system of algebraic equations. The collocation method is subsequently applied to solve this system and determine the unknown coefficients. Finally, error analysis, convergence results based on relevant theorems, and numerical examples are provided to demonstrate the accuracy, reliability, and efficiency of the proposed method.

Keywords. Fractional-order Fibonacci wavelets, Fibonacci polynomial, Taylor expansion, Collocation method, Operational matrices.

MSC. 35R11; 34B10.

How to Cite
Karimi, Sh. Shivanian, E., Barikbin, Z. (2026). "The solution of variable-order fractional integro-differential equations by two-dimensional Fractional-order Fibonacci wavelets operational matrix". *Control and Optimization in Applied Mathematics*, 11(-): 1-27, doi: 10.30473/coam.2026.76466.1358

1 Introduction

Fractional integral and derivative operators have emerged as indispensable tools for modeling and analyzing a wide range of scientific phenomena. These operators are extensively employed across diverse disciplines, including medicine, viscoelastic material dynamics, signal processing, economics, earthquake modeling, electrochemistry, and solid mechanics [1, 7, 8, 10, 11, 14, 21, 24, 31, 50, 53]. A key advantage of fractional calculus is its ability to provide more accurate and realistic descriptions of complex systems compared to classical integer-order models. Over the past decades, several definitions of fractional derivatives have been introduced, notably the Riemann–Liouville [8], Caputo [53], Riesz [4], and Riesz–Feller [4] formulations. Considerable research effort has been devoted to solving fractional differential equations (FDEs), fractional integro-differential equations (FIDEs), and fractional partial differential equations (FPDEs) through various numerical and analytical approaches. Among the computational strategies developed for this purpose are fractional Chebyshev cardinal wavelets [16], Müntz–Legendre hybrid functions [41], Bernstein wavelets [34, 35], Fibonacci wavelets [44], modified hat functions [29], and Petrov–Galerkin methods based on Müntz–Legendre polynomials [40]. Furthermore, Firoozjae et al. [13] proposed a Ritz-based approach for solving the Fokker–Planck equation involving Caputo–Fabrizio fractional derivatives.

A significant generalization of classical fractional calculus is provided by variable-order fractional (VOF) operators, in which the order of differentiation or integration varies as a function of time or space. This extension substantially enriches the modeling capabilities of fractional calculus by allowing nonconstant orders, thereby capturing more nuanced nonlocal and memory-dependent behaviors [46, 47, 48]. Variable-order derivatives have been formulated in several ways, including the Riemann–Liouville, Marchaud, Coimbra, and Grünwald definitions [5, 51]. The flexibility of VOF operators has led to their successful application in mechanics, optimization, physics, and related fields [6, 17, 27, 38, 39, 52, 56]. However, owing to the inherent complexity of VOF systems, closed-form analytical solutions are generally unavailable, which necessitates the development of reliable numerical methods. In this direction, Shekari et al. [49] employed a meshless approach to solve VOF advection–diffusion equations, while Legendre wavelets were used in [20] to handle variable-coefficient VOF equations. Additional numerical techniques include compact finite difference schemes [3], Lagrange scaling functions [42], reproducing kernel theory [22], tau-collocation methods [43], local radial basis function collocation schemes [54], shifted Chebyshev polynomial-based optimization schemes [15], parametric quintic splines [28], and discretization methods for VOF Van der Pol oscillators [26].

Wavelet-based methods have gained considerable prominence in numerical analysis owing to their distinctive properties, such as compact support, multiresolution analysis, and orthogonality. In recent years, the combination of fractional calculus with wavelet techniques has attracted sustained attention due to the strong capability of these methods in modeling memory and nonlocal phenomena. In particular, wavelet-based approaches integrated with operational matrices have proven highly effective for solving fractional differential, integro-differential, and partial differential equations, offering improved accuracy and reduced computational complexity. Furthermore, recent studies have underscored the effectiveness of variable-order fractional models in capturing intricate physical behaviors, stimulating renewed interest in designing robust numerical solvers based on wavelet and spectral techniques. These developments confirm that wavelet-based fractional methods constitute an active and rapidly evolving research area. Notable applications include the Lane–Emden equation via orthonormal Bernoulli wavelets [32], fractional optimal control problems using Bernstein wavelets [33], Bratu-type equations via Taylor wavelets [23, 25], fractional Volterra–Fredholm integro-differential equations using Chebyshev wavelets [57], fractional pantograph differential equations via Müntz–Legendre wavelets [36], and distributed-order FDEs using Chelyshkov wavelets [19]. Legendre wavelets have also been applied to solve the VOF Poisson equation [37], further demonstrating their versatility. Fibonacci wavelets (FWs) constitute a distinct class of wavelets that, although not orthogonal, admit operational matrices (OMs) for integration and differentiation, rendering them highly effective for approximating smooth and piecewise smooth functions. The authors of [45] introduced FWs and derived their integral and delay OMs, which have since been applied to time-varying delay equations and optimal control problems. In addition, two-dimensional Fibonacci wavelets have been proposed for solving fractional Black–Scholes equations arising in financial mathematics [44].

The present study aims to investigate the application of fractional-order Fibonacci wavelets (FOFWs) to the numerical solution of variable-order fractional integro-differential equations (VOFIDEs). By exploiting the distinctive properties of FOFWs, we develop a robust and efficient numerical framework that as confirmed by the convergence analysis and numerical results in Sections 6 and 7. The main novelty of this work lies in the construction of FOFWs and the derivation, for the first time, of their associated operational matrices for variable-order fractional integration and differentiation. These newly developed matrices are systematically combined with a collocation technique to convert the original VOFIDEs into tractable systems of algebraic equations. Compared with existing wavelet-based approaches that rely on classical orthogonal bases such as Chebyshev or Legendre wavelets, the proposed method offers greater flexibility in handling variable-order operators, reduced computational complexity, and superior approximation accuracy, as confirmed by the convergence analysis and numerical experiments presented herein.

The remainder of this paper is organized as follows. Section 2 provides the necessary preliminary definitions and mathematical background. Section 3 introduces the fractional-order Fibonacci wavelets (FOFWs) and their fundamental properties, including function approximation. Section 4 is devoted to the construction of the operational matrices for integration and variable-order fractional differentiation corresponding to the FOFW basis. Section 5 describes the numerical implementation of the proposed collocation method for solving variable-order fractional integro-differential equations. Section 6 presents the convergence analysis of the proposed scheme along with the associated theoretical proofs. Section 7 contains several numerical examples that validate the accuracy and effectiveness of the proposed approach. Section 8 presents the algorithmic procedure for computing the FOFW coefficients and reconstructing the approximate solution. Finally, Section 9 summarizes the main findings and outlines directions for future research.

2 Preliminaries and Basic Definitions

Variable-order fractional calculus has undergone rapid development in recent decades, offering a powerful generalization of classical fractional calculus in which the order of differentiation or integration is permitted to vary as a function of one or more independent variables. In this section, we recall the fundamental definitions and key properties of fractional calculus that are essential for the subsequent development of the proposed method.

Definition 1. The variable-order Caputo fractional derivative of $u(x,t)$ with respect to x is defined as [18, 55]

$$D_x^{q(x,t)}u(x,t) = \frac{1}{\Gamma(\gamma - q(x,t))}\int_0^x (x-s)^{\gamma-q(x,t)-1}\frac{\partial^\gamma u(s,t)}{\partial s^\gamma}\,\mathrm{d}s,$$

where $\gamma - 1 < q(x,t) \leqslant \gamma$, $x > 0$, and $\gamma \in \mathbb{N}$.

This operator satisfies the following useful property:

$$D_x^{q(x,t)}x^\alpha = \begin{cases} \dfrac{\Gamma(\alpha+1)}{\Gamma(\alpha - q(x,t)+1)}x^{\alpha-q(x,t)}, & \gamma \leqslant \alpha, \quad \alpha \in \mathbb{N}, \\ 0, & \text{otherwise.} \end{cases}$$

Remark 1. When the order $q(x,t) = q$ is constant, the variable-order Caputo derivative reduces to the classical Caputo fractional derivative of order q. Furthermore, for $q(x,t) \to \gamma$, the operator recovers the standard integer-order partial derivative $\partial^\gamma/\partial x^\gamma$.

Definition 2 (Generalized Taylor's Formula [30])**.** Let $D^{i\alpha}g(x) \in C(0,1]$ for $i = 0,1,\ldots,m_1$. Then the following expansion holds:

$$g(x) = \sum_{i=0}^{m_1-1}\frac{x^{i\alpha}}{\Gamma(i\alpha+1)}D^{i\alpha}g(0^+) + \frac{x^{m_1\alpha}}{\Gamma(m_1\alpha+1)}D^{m_1\alpha}g(\xi), \tag{1}$$

for some $0 < \xi \leqslant x$, and for all $x \in (0,1]$. Moreover, the following error bound holds:

$$\left| g(x) - \sum_{i=0}^{m_1-1} \frac{x^{i\alpha}}{\Gamma(i\alpha+1)} D^{i\alpha} g(0^+) \right| \leqslant M_\alpha \frac{x^{m_1\alpha}}{\Gamma(m_1\alpha+1)}, \tag{2}$$

where $M_\alpha \geqslant \sup_{\xi\in(0,1]} |D^{m_1\alpha} g(\xi)|$. When $\alpha = 1$, the generalized Taylor's formula reduces to its classical integer-order form.

3 Fractional-Order Fibonacci Wavelets

In this section, we introduce Fibonacci functions and develop the fractional-order Fibonacci wavelets (FOFWs) along with their essential properties.

3.1 Fibonacci Functions

Definition 3. For any $k_1 \in \mathbb{R}^+$, the recurrence relation of the k_1-Fibonacci sequence is defined as [12]

$$\bar{Fib}_{k_1,n_1+1} = k\,\bar{Fib}_{k_1,n_1} + \bar{Fib}_{k_1,n_1-1}, \quad n_1 \geq 1, \tag{3}$$

with initial values $\bar{Fib}_{k_1,0} = 0$ and $\bar{Fib}_{k_1,1} = 1$.

When k_1 is treated as a real variable in Equation (3), we write $\bar{Fib}_{k_1,n_1} = \bar{Fib}_{x,n_1}$. Accordingly, the general recurrence relation for the Fibonacci functions takes the form [12]:

$$\bar{Fib}_{n_1}(x) = \begin{cases} 0, & n_1 = 0, \\ 1, & n_1 = 1, \\ x\,\bar{Fib}_{n_1-1}(x) + \bar{Fib}_{n_1-2}(x), & n_1 > 1. \end{cases} \tag{4}$$

The explicit power series representation of these functions is given by

$$\bar{Fib}_{n_1}(x) = \sum_{i=0}^{\lfloor \frac{n_1-1}{2} \rfloor} \binom{n_1-i-1}{i} x^{n_1-2i-1}, \quad n_1 \geq 1, \tag{5}$$

and their matrix form is expressed as

$$\bar{Fib}(x) = B\,T(x), \tag{6}$$

where

$$\bar{Fib}(x) = \left[\bar{Fib}_0(x), \bar{Fib}_1(x), \bar{Fib}_2(x), \ldots\right]^T, \qquad T(x) = \left[0, 1, x, x^2, x^3, \ldots\right]^T,$$

and B is the coefficient matrix

$$B = \begin{bmatrix} 0 & 0 & 0 & 0 & 0 & 0 & 0 & 0 & \cdots \\ 0 & 1 & 0 & 0 & 0 & 0 & 0 & 0 & \cdots \\ 0 & 0 & 1 & 0 & 0 & 0 & 0 & 0 & \cdots \\ 0 & 1 & 0 & 1 & 0 & 0 & 0 & 0 & \cdots \\ 0 & 0 & 2 & 0 & 1 & 0 & 0 & 0 & \cdots \\ 0 & 1 & 0 & 3 & 0 & 1 & 0 & 0 & \cdots \\ 0 & 0 & 3 & 0 & 4 & 0 & 1 & 0 & \cdots \\ 0 & 1 & 0 & 6 & 0 & 5 & 0 & 1 & \cdots \\ \vdots & \vdots & \vdots & \vdots & \vdots & \vdots & \vdots & \vdots & \ddots \end{bmatrix}.$$

3.2 Fractional-Order Fibonacci Wavelets

For $x \in [0,1]$, $n_1 = 1, 2, \ldots, 2^{k_1-1}$, and $m_1 = 0, 1, \ldots, M-1$, the Fibonacci wavelets are defined as

$$\psi_{n_1,m_1}(x) = \begin{cases} \dfrac{2^{\frac{k_1-1}{2}}}{\sqrt{\omega_{m_1+1}}} F\bar{i}b_{m_1+1}\left(2^{k_1-1}x - n_1 + 1\right), & x \in \left[\dfrac{n_1-1}{2^{k_1-1}}, \dfrac{n_1}{2^{k_1-1}}\right), \\ 0, & \text{otherwise}, \end{cases} \tag{7}$$

where $\omega_{m_1} = \int_0^1 F\bar{i}b_{m_1}^2(x)\,\mathrm{d}x$. To illustrate, for $k_1 = 2$ and $M = 3$, these functions are explicitly given by

$$\psi_{1,0}(x) = \begin{cases} \sqrt{2}, & x \in \left[0, \frac{1}{2}\right), \\ 0, & \text{otherwise}, \end{cases} \qquad \psi_{2,0}(x) = \begin{cases} \sqrt{2}, & x \in \left[\frac{1}{2}, 1\right), \\ 0, & \text{otherwise}, \end{cases}$$

$$\psi_{1,1}(x) = \begin{cases} 2\sqrt{6}\,x, & x \in \left[0, \frac{1}{2}\right), \\ 0, & \text{otherwise}, \end{cases} \qquad \psi_{2,1}(x) = \begin{cases} \sqrt{6}(2x-1), & x \in \left[\frac{1}{2}, 1\right), \\ 0, & \text{otherwise}, \end{cases}$$

$$\psi_{1,2}(x) = \begin{cases} \sqrt{\frac{15}{14}}(1+4x^2), & x \in \left[0, \frac{1}{2}\right), \\ 0, & \text{otherwise}, \end{cases} \qquad \psi_{2,2}(x) = \begin{cases} \sqrt{\frac{30}{7}}(2x^2-2x+1), & x \in \left[\frac{1}{2}, 1\right), \\ 0, & \text{otherwise}. \end{cases}$$

By applying the substitution $x \mapsto x^\alpha$ with $\alpha > 0$, the fractional-order Fibonacci wavelets (FOFWs) are obtained and denoted by $\psi^\alpha_{n_1 m_1}(x)$. The two-dimensional FOFWs are then defined as the tensor product

$$\psi^{\alpha\beta}_{n_1 m_1 n_2 m_2}(x,t) = \psi^\alpha_{n_1 m_1}(x)\,\psi^\beta_{n_2 m_2}(t).$$

Furthermore, the integral of the one-dimensional FOFW over $[0,1]$ is given by

$$\int_0^1 \psi^{\alpha}_{n_1,m_1}(x)\,\mathrm{d}x = \int_0^1 \frac{2^{\frac{k_1-1}{2}}}{\sqrt{\omega_{m_1+1}}} \bar{Fib}_{m_1+1}\left(2^{k_1-1}x^{\alpha} - n_1 + 1\right)\mathrm{d}x$$
$$= \int_0^1 \left(\frac{2^{\frac{k_1-1}{2}}}{\sqrt{\omega_{m_1+1}}} \sum_{i=0}^{\lfloor \frac{m_1}{2} \rfloor} \binom{m_1-i}{i} \left(2^{k_1-1}x^{\alpha} - n_1 + 1\right)^{m_1-2i} \right)\mathrm{d}x$$
$$= \frac{2^{\frac{k_1-1}{2}}}{\sqrt{\omega_{m_1+1}}} \sum_{i=0}^{\lfloor \frac{m_1}{2} \rfloor} \sum_{r=0}^{m_1-2i} \binom{m_1-i}{i} \binom{m_1-2i}{r} 2^{(k_1-1)r}(1-n_1)^{m_1-2i-r} \int_0^1 x^{\alpha r}\,\mathrm{d}x$$
$$= \frac{2^{\frac{k_1-1}{2}}}{\sqrt{\omega_{m_1+1}}} \sum_{i=0}^{\lfloor \frac{m_1}{2} \rfloor} \sum_{r=0}^{m_1-2i} \binom{m_1-i}{i} \binom{m_1-2i}{r} 2^{(k_1-1)r} \frac{(1-n_1)^{m_1-2i-r}}{\alpha r + 1} \times$$
$$\left[\left(\frac{n_1}{2^{k_1-1}} \right)^{\alpha r+1} - \left(\frac{n_1-1}{2^{k_1-1}} \right)^{\alpha r+1} \right].$$

3.3 Function Approximation

Any continuous and bounded function $g(x,t) \in L^2([0,1) \times [0,1))$ can be approximated by the two-dimensional FOFWs as

$$\begin{aligned} g(x,t) \simeq \hat{g}(x,t) &= \sum_{n_1=1}^{2^{k_1-1}} \sum_{n_2=1}^{2^{k_2-1}} \sum_{m_1=0}^{M_1-1} \sum_{m_2=0}^{M_2-1} a_{n_1m_1n_2m_2}\, \psi^{\alpha\beta}_{n_1m_1n_2m_2}(x,t) \\ &= \psi^{\alpha T}_{n_1m_1}(x)\, A\, \psi^{\beta T}_{n_2m_2}(t), \end{aligned} \tag{8}$$

where the coefficient matrix A is determined by

$$A = Q^{-1} \langle \langle g(x,t), \psi^{\alpha}_{n_1m_1}(x) \rangle, \psi^{\beta}_{n_2m_2}(t) \rangle\, \hat{Q}^{-1},$$

and the basis vectors and Gram matrices are defined as

$$\psi^{\alpha}_{n_1m_1}(x) = \left[\psi^{\alpha}_{1,0}(x),\, \psi^{\alpha}_{1,1}(x),\, \dots,\, \psi^{\alpha}_{1,M_1-1}(x),\, \psi^{\alpha}_{2,0}(x),\, \dots,\, \psi^{\alpha}_{2^{k_1-1},M_1-1}(x)\right]^T,$$
$$\psi^{\beta}_{n_2m_2}(t) = \left[\psi^{\beta}_{1,0}(t),\, \psi^{\beta}_{1,1}(t),\, \dots,\, \psi^{\beta}_{1,M_2-1}(t),\, \psi^{\beta}_{2,0}(t),\, \dots,\, \psi^{\beta}_{2^{k_2-1},M_2-1}(t)\right]^T,$$
$$Q = \left\langle \psi^{\alpha}_{n_1m_1}(x), \psi^{\alpha}_{n_1m_1}(x) \right\rangle = \int_0^1 \psi^{\alpha}_{n_1m_1}(x)\, \psi^{\alpha T}_{n_1m_1}(x)\, x^{\alpha-1}\,\mathrm{d}x,$$
$$\hat{Q} = \left\langle \psi^{\beta}_{n_2m_2}(t), \psi^{\beta}_{n_2m_2}(t) \right\rangle = \int_0^1 \psi^{\beta}_{n_2m_2}(t)\, \psi^{\beta T}_{n_2m_2}(t)\, t^{\beta-1}\,\mathrm{d}t.$$

Once the function $g(x,t)$ and the parameters $k_1,\ k_2,\ M_1,\ M_2$ are specified, the matrices A, Q, and $\hat{Q}$ are fully determined. For instance, taking $g(x,t) = xt$, $\alpha = \beta = 1$, $k_1 = k_2 = 1$, and $M_1 = M_2 = 2$, one obtains

$$\psi^{\alpha}_{n_1m_1}(x) = [1,\ \sqrt{3}\,x]^T, \qquad \psi^{\beta}_{n_2m_2}(t) = [1,\ \sqrt{3}\,t]^T,$$

$$Q = \hat{Q} = \begin{bmatrix} 1 & \frac{\sqrt{3}}{2} \\ \frac{\sqrt{3}}{2} & 1 \end{bmatrix}, \qquad Q^{-1} = \hat{Q}^{-1} = \begin{bmatrix} 4 & -2\sqrt{3} \\ -2\sqrt{3} & 4 \end{bmatrix},$$

which yields

$$A = \begin{bmatrix} 0 & 0 \\ 0 & \frac{1}{3} \end{bmatrix}.$$

Substituting these matrices into (8) confirms that $\hat{g}(x,t) = g(x,t) = xt$, demonstrating the exactness of the approximation in this case.

4 Operational Matrices

In this section, we derive and present two key operational matrices (OMs) associated with the FOFW basis: the integral OM and the OM of the variable-order fractional derivative (VOFD). These matrices are central to the numerical implementation developed in Section 5.

4.1 Integral Operational Matrix

The integral of the basis vector $\psi^{\alpha}_{n_1 m_1}(x)$ may be approximated as

$$\int_0^x \psi^{\alpha}_{n_1 m_1}(\varsigma)\, \mathrm{d}\varsigma \simeq \Theta_\alpha\, \psi^{\alpha}_{n_1 m_1}(x), \tag{9}$$

where Θ_α is the integral OM. To derive its entries, we expand the FOFW using the power series representation in (5):

$$\int_0^x \psi^{\alpha}_{n_1 m_1}(\varsigma)\, \mathrm{d}\varsigma = \int_0^x \frac{2^{\frac{k_1-1}{2}}}{\sqrt{\omega_{m_1+1}}} F\bar{i}b_{m_1+1}\left(2^{k_1-1}\varsigma^{\alpha} - n_1 + 1\right) \mathrm{d}\varsigma$$

$$= \int_0^x \frac{2^{\frac{k_1-1}{2}}}{\sqrt{\omega_{m_1+1}}} \left(\sum_{i=0}^{\lfloor \frac{m_1}{2} \rfloor} \binom{m_1 - i}{i} \left(2^{k_1-1}\varsigma^{\alpha} - n_1 + 1\right)^{m_1 - 2i} \right) \mathrm{d}\varsigma$$

$$= \frac{2^{\frac{k_1-1}{2}}}{\sqrt{\omega_{m_1+1}}} \sum_{i=0}^{\lfloor \frac{m_1}{2} \rfloor} \sum_{\kappa=0}^{m_1-2i} \binom{m_1 - i}{i} \binom{m_1 - 2i}{\kappa} 2^{(k_1-1)\kappa} (1 - n_1)^{m_1 - 2i - \kappa} \int_0^x \varsigma^{\alpha\kappa}\, \mathrm{d}\varsigma,$$

where, according to the support of the wavelets, the integral of $\varsigma^{\alpha\kappa}$ is given by

$$\int_0^x \varsigma^{\alpha\kappa}\,\mathrm{d}\varsigma = \begin{cases} 0, & x < \dfrac{n_1-1}{2^{k_1-1}}, \\[2ex] \dfrac{1}{\alpha\kappa+1}\left[x^{\alpha\kappa+1} - \left(\dfrac{n_1-1}{2^{k_1-1}}\right)^{\alpha\kappa+1}\right], & \dfrac{n_1-1}{2^{k_1-1}} \le x < \dfrac{n_1}{2^{k_1-1}}, \\[2ex] \dfrac{1}{\alpha\kappa+1}\left[\left(\dfrac{n_1}{2^{k_1-1}}\right)^{\alpha\kappa+1} - \left(\dfrac{n_1-1}{2^{k_1-1}}\right)^{\alpha\kappa+1}\right], & x \ge \dfrac{n_1}{2^{k_1-1}}. \end{cases}$$

As a concrete illustration, for $M_1 = 5$ and $k_1 = 1$, the individual integral approximations are

$$\int_0^x \psi_{10}^{\alpha}(\varsigma)\,\mathrm{d}\varsigma = \left[0,\ \tfrac{1}{\sqrt{3}},\ 0,\ 0,\ 0\right]\psi^{\alpha}(x),$$
$$\int_0^x \psi_{11}^{\alpha}(\varsigma)\,\mathrm{d}\varsigma = \left[-\tfrac{\sqrt{3}}{2},\ 0,\ \sqrt{\tfrac{7}{5}},\ 0,\ 0\right]\psi^{\alpha}(x),$$
$$\int_0^x \psi_{12}^{\alpha}(\varsigma)\,\mathrm{d}\varsigma = \left[0,\ \tfrac{\sqrt{5}}{6\sqrt{7}},\ 0,\ \tfrac{\sqrt{239}}{42},\ 0\right]\psi^{\alpha}(x),$$
$$\int_0^x \psi_{13}^{\alpha}(\varsigma)\,\mathrm{d}\varsigma = \left[-\tfrac{\sqrt{105}}{2\sqrt{239}},\ 0,\ \tfrac{7}{2\sqrt{239}},\ 0,\ \tfrac{\sqrt{1943}}{4\sqrt{717}}\right]\psi^{\alpha}(x),$$
$$\int_0^x \psi_{14}^{\alpha}(\varsigma)\,\mathrm{d}\varsigma = \left[0,\ 0,\ 0,\ \tfrac{\sqrt{717}}{5\sqrt{1943}},\ 0\right]\psi^{\alpha}(x),$$

so that the integral OM takes the form

$$\Theta_\alpha = \begin{bmatrix} 0 & \dfrac{1}{\sqrt{3}} & 0 & 0 & 0 \\ -\dfrac{\sqrt{3}}{2} & 0 & \sqrt{\dfrac{7}{5}} & 0 & 0 \\ 0 & \dfrac{\sqrt{5}}{6\sqrt{7}} & 0 & \dfrac{\sqrt{239}}{42} & 0 \\ -\dfrac{\sqrt{105}}{2\sqrt{239}} & 0 & \dfrac{7}{2\sqrt{239}} & 0 & \dfrac{\sqrt{1943}}{4\sqrt{717}} \\ 0 & 0 & 0 & \dfrac{\sqrt{717}}{5\sqrt{1943}} & 0 \end{bmatrix}. \tag{10}$$

Figure 1 illustrates the exact and approximate integrals of $\psi_{n_1 m_1}^{\alpha}(x)$ for $M_1 = 5$ and $k_1 = 1$, confirming the accuracy of the approximation in (9).

More generally, the r-fold iterated integral of $\psi_{n_1 m_1}^{\alpha}(x)$ satisfies

$$\underbrace{\int_0^x \int_0^x \cdots \int_0^x}_{r \text{ times}} \psi_{n_1 m_1}^{\alpha}(\varsigma)\,\mathrm{d}\varsigma \cdots \mathrm{d}\varsigma \simeq \Theta_\alpha^r\, \psi_{n_1 m_1}^{\alpha}(x), \qquad r = 1, 2, \ldots, n. \tag{11}$$

4.2 Operational Matrix of Variable-Order Fractional Derivative

We now construct the OM of the VOFD, denoted Ω_q^{α}, defined by the approximation

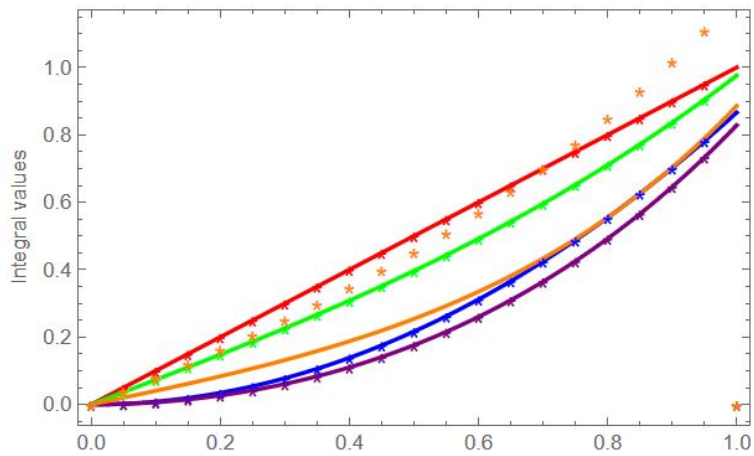

Figure 1: Exact and approximate integral of $\psi^{\alpha}_{n_1 m_1}(x)$ for $M_1 = 5$ and $k_1 = 1$.

$$D_x^{q(x,t)}\big(\psi^{\alpha}_{n_1 m_1}(x)\big) \simeq \Omega^{\alpha}_q\, \psi^{\alpha}_{n_1 m_1}(x), \quad 0 < q(x,t) \le 1, \tag{12}$$

where Ω^{α}_q is a $2^{k_1-1}M_1 \times 2^{k_1-1}M_1$ matrix depending on $q(x,t)$. To derive an explicit form, we introduce the auxiliary basis

$$\rho_i(x) = x^{\alpha(i-1)}, \quad i = 1, 2, \ldots, 2^{k_1-1}M_1, \tag{13}$$

and define the vector

$$\Phi(x) = \big[\rho_1(x),\ \rho_2(x),\ \ldots,\ \rho_{2^{k_1-1}M_1}(x)\big]^T. \tag{14}$$

This vector is related to the FOFW basis by

$$\Phi(x) \cong \Lambda\, \psi^{\alpha}_{n_1 m_1}(x), \tag{15}$$

where Λ is the change-of-basis matrix. For $M_1 = 5$ and $k_1 = 1$, this matrix is explicitly given by

$$\Lambda = \begin{bmatrix} 1 & 0 & 0 & 0 & 0 \\ 0 & \dfrac{1}{\sqrt{3}} & 0 & 0 & 0 \\ -1 & 0 & 2\sqrt{\dfrac{7}{15}} & 0 & 0 \\ 0 & \dfrac{-2}{\sqrt{3}} & 0 & \sqrt{\dfrac{239}{105}} & 0 \\ 2 & 0 & -6\sqrt{\dfrac{7}{15}} & 0 & \dfrac{1}{3}\sqrt{\dfrac{1943}{35}} \end{bmatrix}.$$

Applying the variable-order Caputo fractional derivative to $\Phi(x)$ and using the property recalled in Section 2, we obtain

$$D_x^{q(x,t)}(\Phi(x)) \cong F^x_{q(x,t)}\,\Phi(x), \quad 0 < q(x,t) \leq 1, \tag{16}$$

where $F^x_{q(x,t)}$ is the $2^{k_1-1}M_1 \times 2^{k_1-1}M_1$ diagonal matrix

$$F^x_{q(x,t)} = \frac{1}{x^{q(x,t)}} \times \begin{bmatrix} 0 & 0 & 0 & \cdots & 0 & 0 \\ 0 & \frac{\Gamma(\alpha+1)}{\Gamma(\alpha+1-q(x,t))} & 0 & \cdots & 0 & 0 \\ 0 & 0 & \frac{\Gamma(2\alpha+1)}{\Gamma(2\alpha+1-q(x,t))} & \cdots & 0 & 0 \\ \vdots & \vdots & \vdots & \ddots & 0 & 0 \\ 0 & 0 & 0 & \cdots & \frac{\Gamma((2^{k_1-1}M_1-2)\alpha+1)}{\Gamma((2^{k_1-1}M_1-2)\alpha+1-q(x,t))} & 0 \\ 0 & 0 & 0 & \cdots & 0 & \frac{\Gamma((2^{k_1-1}M_1-1)\alpha+1)}{\Gamma((2^{k_1-1}M_1-1)\alpha+1-q(x,t))} \end{bmatrix}.$$

Finally, combining Equations (15) and (16), the VOFD OM is obtained as

$$D_x^{q(x,t)}\left(\psi^\alpha_{n_1m_1}(x)\right) \simeq \Omega^\alpha_q\,\psi^\alpha_{n_1m_1}(x) = \left(\Lambda^{-1}F^x_{q(x,t)}\Lambda\right)\psi^\alpha_{n_1m_1}(x). \tag{17}$$

5 Method Implementation

In this section, we present the implementation of the proposed method for VOFPIDEs. We consider the following nonlinear variable-order fractional partial integro-differential equation on the domain $[0,1]\times[0,1]$, with $0 < q(x,t) \leqslant 1$:

$$D_t^{q(x,t)}u(x,t) + \sum_{k=0}^{2} p_k(x,t)\frac{\partial^k u(x,t)}{\partial x^k} = H(x,t) + \rho\int_0^t K(x,t,\eta)O(x,\eta,u(x,\eta))\mathrm{d}\eta, \tag{18}$$

with the initial condition

$$u(x,0) = f(x), \quad x \in [0,1], \tag{19}$$

and the boundary conditions

$$u(0,t) = W_0(t), \quad u(1,t) = W_1(t), \quad t \in [0,1]. \tag{20}$$

Here, ρ, $H(x,t)$, $K(x,t,\eta)$, $p_k(x,t)$, $f(x)$, $W_0(t)$, and $W_1(t)$ are known functions, while $u(x,t)$ is the unknown function. Moreover, $D_t^{q(x,t)}u(x,t)$ denotes the Caputo fractional derivative of order $q(x,t)$.

To approximate Equation (18), we assume

$$\frac{\partial^3 u(x,t)}{\partial x^2 \partial t} \cong \psi^{\alpha T}_{n_1m_1}(x)\hat{P}\psi^\beta_{n_2m_2}(t), \tag{21}$$

where

$$\hat{P} = [\hat{p}_{ij}], \quad i = 1, 2, \ldots, 2^{k_1-1}M_1, \quad j = 1, 2, \ldots, 2^{k_2-1}M_2. \tag{22}$$

Integrating (21) with respect to t, we obtain

$$\frac{\partial^2 u(x,t)}{\partial x^2} \cong \psi^{\alpha T}_{n_1 m_1}(x)\hat{P}\Theta_\beta \psi^\beta_{n_2 m_2}(t) + f''(x). \tag{23}$$

Next, by performing two successive integrations of Equation (23) with respect to x over the interval $[0, x]$, we derive

$$\frac{\partial u(x,t)}{\partial x} \cong \psi^{\alpha T}_{n_1 m_1}(x)\Theta^T_\alpha \hat{P}\Theta_\beta \psi^\beta_{n_2 m_2}(t) + f'(x) - f'(0) + \frac{\partial u(0,t)}{\partial x}, \tag{24}$$

and

$$u(x,t) \cong \psi^{\alpha T}_{n_1 m_1}(x)(\Theta^2_\alpha)^T \hat{P}\Theta_\beta \psi^\beta_{n_2 m_2}(t) + f(x) - f(0) - x f'(0) + x\frac{\partial u(0,t)}{\partial x} + W_0(t). \tag{25}$$

By integrating Equation (24) with respect to x over $[0, 1]$, we approximate $\frac{\partial u(0,t)}{\partial x}$ as follows:

$$\frac{\partial u(0,t)}{\partial x} \cong f(0) - f(1) + f'(0) - W_0(t) + W_1(t) - R_{n_1 m_1}\big(\Theta^T_\alpha \hat{P}\Theta_\beta \psi^\beta_{n_2 m_2}(t)\big), \tag{26}$$

where

$$R_{n_1 m_1} = \int_0^1 \psi^{\alpha T}_{n_1 m_1}(x)\mathrm{d}x.$$

Substituting (26) into (24) and (25), we obtain

$$\begin{aligned}\frac{\partial u(x,t)}{\partial x} \cong{}& \psi^{\alpha T}_{n_1 m_1}(x)\Theta^T_\alpha \hat{P}\Theta_\beta \psi^\beta_{n_2 m_2}(t) + f'(x) + W_1(t) - W_0(t)\\ &+ f(0) - f(1) - R_{n_1 m_1}\big(\Theta^T_\alpha \hat{P}\Theta_\beta \psi^\beta_{n_2 m_2}(t)\big),\end{aligned} \tag{27}$$

and

$$\begin{aligned}u(x,t) \cong{}& \psi^{\alpha T}_{n_1 m_1}(x)(\Theta^2_\alpha)^T \hat{P}\Theta_\beta \psi^\beta_{n_2 m_2}(t) + f(x) - f(0) - x f(1) + x f(0)\\ &+ x W_1(t) + (1-x)W_0(t) - x\big(R_{n_1 m_1}(\Theta^T_\alpha \hat{P}\Theta_\beta \psi^\beta_{n_2 m_2}(t))\big)\\ ={}& u_{n_1 m_1 n_2 m_2}(x,t).\end{aligned} \tag{28}$$

To solve Equation (18), it is necessary to evaluate $D^{q(x,t)}_t u(x,t)$. Using (28), we obtain

$$\begin{aligned}D^{q(x,t)}_t u(x,t) \cong{}& \psi^{\alpha T}_{n_1 m_1}(x)(\Theta^2_\alpha)^T \hat{P}\Theta_\beta D^{q(x,t)}_t \psi^\beta_{n_2 m_2}(t) + x D^{q(x,t)}_t W_1(t)\\ &+ (1-x)D^{q(x,t)}_t W_0(t) - x\big(R_{n_1 m_1}(\Theta^T_\alpha \hat{P}\Theta_\beta D^{q(x,t)}_t \psi^\beta_{n_2 m_2}(t))\big).\end{aligned} \tag{29}$$

Finally, using Equations (23), (29), and (18), we obtain

$$D_t^{q(x,t)}u(x,t)+\sum_{k=0}^{2}p_k(x,t)\frac{\partial^k u(x,t)}{\partial x^k}\cong\psi_{n_1m_1}^{\alpha T}(x)(\Theta_\alpha^2)^T\hat{P}\Theta_\beta(\Lambda^{-1}F_{q(x,t)}^t\Lambda)\psi_{n_2m_2}^\beta(t)$$
$$+xD_t^{q(x,t)}W_1(t)+(1-x)D_t^{q(x,t)}W_0(t)$$
$$-x(R_{n_1m_1}(\Theta_\alpha^T\hat{P}\Theta_\beta(\Lambda^{-1}F_{q(x,t)}^t\Lambda)\psi_{n_2m_2}^\beta(t)))$$
$$+p_0(x,t)\Big(\psi_{n_1m_1}^{\alpha T}(x)(\Theta_\alpha^2)^T\hat{P}\Theta_\beta\psi_{n_2m_2}^\beta(t)$$
$$+f(x)-f(0)-xf(1)+xf(0)$$
$$+xW_1(t)+(1-x)W_0(t)-x(R_{n_1m_1}(\Theta_\alpha^T\hat{P}\Theta_\beta\psi_{n_2m_2}^\beta(t)))\Big)$$
$$+\ p_1(x,t)\Big(\psi_{n_1m_1}^{\alpha T}(x)\Theta_\alpha^T\hat{P}\Theta_\beta\psi_{n_2m_2}^\beta(t)$$
$$+f'(x)+W_1(t)-W_0(t)$$
$$+f(0)-f(1)-R_{n_1m_1}(\Theta_\alpha^T\hat{P}\Theta_\beta\psi_{n_2m_2}^\beta(t))\Big)$$
$$+p_2(x,t)\Big(\psi_{n_1m_1}^{\alpha}(x)\hat{P}\Theta_\beta\psi_{n_2m_2}^\beta(t)+f''(x)\Big)=\hat{G}(x,t). \tag{30}$$

Now, assume that

$$O(x,\eta,u(x,\eta))\cong\psi_{n_1m_1}^{\alpha T}(x)\hat{J}\psi_{n_2m_2}^\beta(t), \tag{31}$$

where $\hat{J}$ is an unknown coefficient matrix of the same dimensions as $\hat{P}$.

Next, we approximate the integral term in (18). To maintain tractability within our wavelet-based framework, we assume that the kernel admits a finite separable representation of the form

$$K(x,t,\eta)=\sum_{r=1}^{P}\mu_r(x)\Phi_r(t)\upsilon_r(\eta). \tag{32}$$

This is a standard assumption in wavelet-based methods and, despite being a limitation, is often required to cover a broad class of practical applications. Therefore, the integral term in Equation (18) can be written as

$$\int_0^t K(x,t,\eta)O(x,\eta,u(x,\eta))\mathrm{d}\eta\cong\sum_{r=1}^{P}\mu_r(x)\Phi_r(t)\int_0^t\upsilon_r(\eta)\psi_{n_2m_2}^{\beta T}(\eta)\mathrm{d}\eta\hat{J}^T\psi_{n_1m_1}^{\alpha}(x)$$
$$=\hat{R}(x,t). \tag{33}$$

Thus, from Equations (18), (30), and (33), we obtain

$$\hat{G}(x,t)=H(x,t)+\rho\hat{R}(x,t). \tag{34}$$

Finally, using Equation (34) together with the collocation method, a system of algebraic equations is obtained for the unknown matrices $\hat{J}$ and $\hat{P}$. By substituting $\hat{P}$ into (28), the approximate solution of Equation (18) is obtained.

6 Convergence Analysis

A function $g(x) \in L^2[0,1]$ can be expressed as a uniformly convergent infinite series of FOFWs:

$$g(x) = \sum_{n_1=1}^{\infty} \sum_{m_1=0}^{\infty} b_{n_1,m_1} \psi^{\alpha}_{n_1,m_1}(x).$$

Since the truncated FOFWs series provides an approximation to the solution, the associated error function $E(x)$ is defined as

$$E(x) = \left| g(x) - \sum_{n_1=1}^{2^{k_1-1}} \sum_{m_1=0}^{M-1} b_{n_1,m_1} \psi^{\alpha}_{n_1,m_1}(x) \right|.$$

By evaluating at $x = x_i \in [0,1]$, the absolute error at the point x_i is obtained. The error bound of the approximate solution based on the FOFWs series is given in the following theorem.

Theorem 1. Suppose that $D^{\alpha i} g \in C[0,1)$ for $i = 0, 1, \ldots, M$, with $(2M+1)\alpha \geqslant 1$. Let $\hat{m} = 2^{k_1-1}M$ and $Y^{\alpha}_{M} = \text{span}\{\bar{Fib}^{\alpha}_0(x), \bar{Fib}^{\alpha}_1(x), \ldots, \bar{Fib}^{\alpha}_{M-1}(x)\}$.

If $g_{\hat{m}}(x) = A^T \bar{Fib}^{\alpha}(x)$ is the best approximation to $g(x)$ from Y^{α}_M on the interval $I_{n_1,k_1} = \left[\frac{n_1-1}{2^{k_1-1}}, \frac{n_1}{2^{k_1-1}}\right]$, then the error bound of the approximate solution $g_{\hat{m}}(x)$ using the FOFWs series over $[0,1]$ is given by

$$\|g(x) - g_{\hat{m}}(x)\|_2 \leqslant \frac{\sup_{x\in[0,1]} |D^{M\alpha} g(x)|}{\Gamma(M\alpha+1)\sqrt{(2M+1)\alpha}},$$

where

$$\bar{Fib}^{\alpha}(x) = [\bar{Fib}^{\alpha}_0(x), \bar{Fib}^{\alpha}_1(x), \ldots, \bar{Fib}^{\alpha}_{M-1}(x)]^T.$$

Proof. Define

$$\hat{g}(x) = \sum_{i=0}^{M-1} \frac{x^{\alpha i}}{\Gamma(\alpha i+1)} D^{\alpha i} g(0^+).$$

From the generalized Taylor formula [30], it follows that

$$|g(x) - \hat{g}(x)| \leqslant \frac{x^{\alpha M}}{\Gamma(\alpha M+1)} \sup_{x\in I_{n_1,k_1}} \left| D^{M\alpha} g(x) \right|.$$

Next, using the concept of best approximation and the fact that $\sum_{i=0}^{M-1} \frac{x^{\alpha i}}{\Gamma(\alpha i+1)} D^{\alpha i} g(0^{+}) \in Y_M^{\alpha}$, we obtain

$$\begin{aligned}
\|g(x)-\hat{g}(x)\|^2_{L^2[0,1]} &= \|g(x)-B^T\psi^{\alpha}(x)\|^2_{L^2[0,1]} \\
&= \sum_{n_1=1}^{2^{k_1-1}} \|g(x)-A^T \bar{Fib}^{\alpha}(x)\|^2_{L^2[I_{n_1,k_1}]} \\
&\leqslant \sum_{n_1=1}^{2^{k_1-1}} \|g(x)-\hat{g}(x)\|^2_{L^2[I_{n_1,k_1}]} \\
&\leqslant \sum_{n_1=1}^{2^{k_1-1}} \int_{I_{n_1,k_1}} \left[\sup_{x\in I_{n_1,k_1}} \left|D^{M\alpha} g(x)\right|\right]^2 x^{\alpha-1} dx \\
&\leqslant \int_0^1 \left[\sup_{x\in[0,1]} \left|D^{M\alpha} g(x)\right|\right]^2 x^{\alpha-1} dx \\
&\leqslant \frac{1}{\Gamma(M\alpha+1)^2(2M+1)\alpha} \left[\sup_{x\in[0,1]} \left|D^{M\alpha} g(x)\right|\right]^2 .
\end{aligned}$$

Taking the square root completes the proof. □

7 Numerical Examples

In this section, two examples of VOFPID equations are presented.

Example 1. Assume the following VOFPID equation of Volterra type [9]:

$$D_t^{q(x,t)} u(x,t) + x\frac{\partial u(x,t)}{\partial x} + \frac{\partial^2 u(x,t)}{\partial x^2} = H(x,t) + \rho \int_0^t u(x,\xi) \mathrm{d}\xi, \quad 0 < q(x,t) \leq 1,$$

where

$$H(x,t) = 2t^q + 2x^2 + 2 - \rho\left(x^2 t + \frac{2\Gamma(q+1)}{\Gamma(2q+1)(2q+1)} t^{(2q+1)}\right),$$

with the initial condition

$$u(x,0) = x^2, \quad x \in [0,1],$$

and the boundary conditions

$$u(0,t) = \frac{2\Gamma(q+1)}{\Gamma(2q+1)} t^{2q},$$

$$u(1,t) = 1 + \frac{2\Gamma(q+1)}{\Gamma(2q+1)} t^{2q}, \quad t \in [0,1].$$

The exact solution is

$$u(x,t) = x^2 + \frac{2\Gamma(q+1)}{\Gamma(2q+1)} t^{2q}.$$

A comparison between the exact and approximate solutions is presented in Table 1. In addition, Figures 1 and 2 illustrate the exact and approximate solutions for different parameter values. As shown in Figure 2, the proposed method accurately reproduces the exact solution.

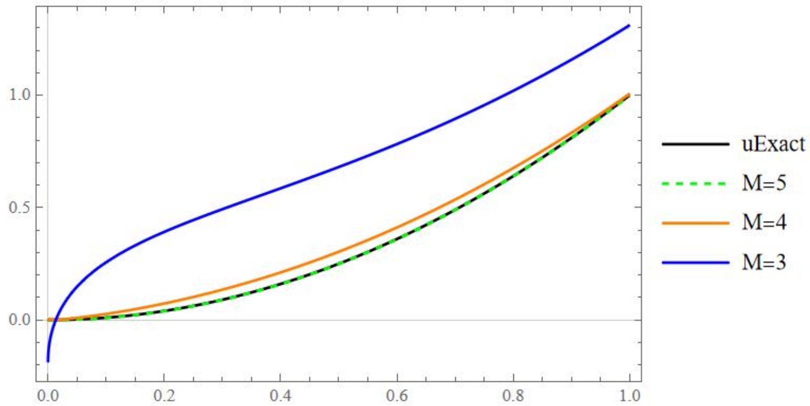

Figure 2: Exact and approximate solutions for $\alpha = \beta = q = 0.5$, $k_1 = k_2 = 1$, and $M_1 = M_2 = 3, 4, 5$ in $(x,t) \in [0,1] \times [0,1]$ of Example 1.

Table 1: Comparison of the exact and approximate solutions for $q(x) = 0.75$, $\alpha = \beta = 1$, $k_1 = k_2 = 1$, and $M_1 = M_2 = 7$ (Example 1).

x	t	**Approximate solution**	**Exact solution**
0	0	$4.300092923096153 \times 10^{-24}$	0*
0.1	0.1	0.053725909824090576	0.053725909824090576
0.2	0.2	0.1636755494006637	0.1636755494006637
0.3	0.3	0.3172064922675	0.31720649226749986
0.4	0.4	0.5098072785927246	0.5098072785927246
0.5	0.5	0.7388705337234619	0.7388705337234619
0.6	0.6	1.0026370056478324	1.0026370056478322
0.7	0.7	1.2998151827120579	1.2998151827120576
0.8	0.8	1.6294043952053097	1.6294043952053097
0.9	0.9	1.9905995652504453	1.9905995652504453
1	1	2.3827346780725867	2.3827346780725867

*The nonzero value at $(0,0)$ is a floating-point artifact of the collocation procedure and is negligible (of order 10^{-24}).

Remark 2.

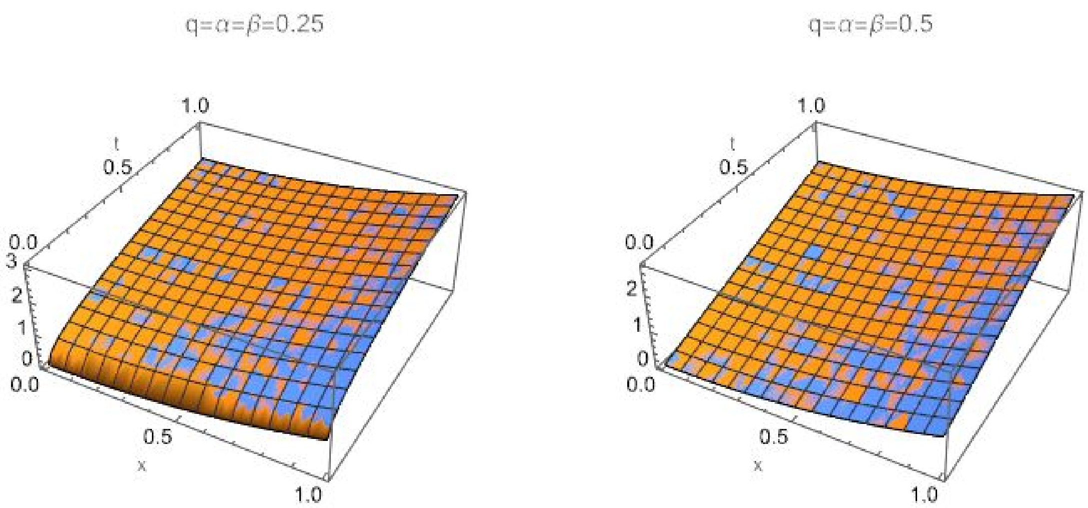

Figure 3: Exact and approximate solutions for $\alpha = \beta = q = 0.25, 0.5$, $k_1 = k_2 = 2$, and $M_1 = M_2 = 4$ in $(x, t) \in [0, 1] \times [0, 1]$ of Example 1.

Example 2. Consider the following nonlinear variable-order fractional partial integro-differential (VOFPID) Volterra equation [2, 9]

$$D_t^{q(x,t)} u(x,t) = H(x,t) + (1+x^2)\frac{\partial^2 u(x,t)}{\partial x^2} + \int_0^t \left(x^2 + t\, u^2(x,\xi)\right) \mathrm{d}\xi, \qquad 0 < q(x,t) \leq 1,$$

subject to the initial condition

$$u(x,0) = \sinh(x) + 1, \quad x \in [0,1],$$

and the boundary conditions

$$u(0,t) = 1,$$
$$u(1,t) = \sinh(1) + e^{-t}, \quad t \in [0,1],$$

where, for $q(x,t) = 1$ and a suitable choice of $H(x,t)$, the exact solution is

$$u(x,t) = \sinh(x) + e^{-xt}.$$

The absolute errors are reported in Table 2, and the exact and approximate solutions are illustrated in Figure 4.

8 Algorithms

In this section, we present the algorithm for the proposed method.

Table 2: Absolute error for $q(x) = 1$, $\alpha = \beta = 1$, $k_1 = k_2 = 1$, and $M_1 = M_2 = 4, 6$ (Example 2).

x	t	$M_1 = M_2 = 4$	$M_1 = M_2 = 6$
0	0	0	0
0.1	0.1	$1.07069536 \times 10^{-1}$	$4.33908054 \times 10^{-4}$
0.2	0.2	$1.91816326 \times 10^{-1}$	$2.95671146 \times 10^{-3}$
0.3	0.3	$2.52889989 \times 10^{-1}$	$8.31428093 \times 10^{-3}$
0.4	0.4	$2.89795317 \times 10^{-1}$	$1.59842294 \times 10^{-2}$
0.5	0.5	$3.02588397 \times 10^{-1}$	$2.44645467 \times 10^{-2}$
0.6	0.6	$2.91517911 \times 10^{-1}$	$3.16106555 \times 10^{-2}$
0.7	0.7	$2.56648925 \times 10^{-1}$	$3.49833184 \times 10^{-2}$
0.8	0.8	$1.97505421 \times 10^{-1}$	$3.21707472 \times 10^{-2}$
0.9	0.9	$1.12761393 \times 10^{-1}$	$2.10546275 \times 10^{-2}$
1	1	0	0

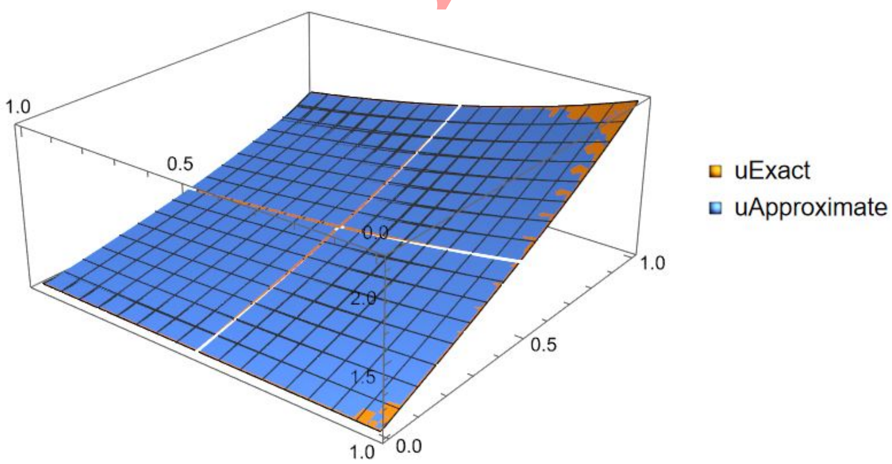

Figure 4: Exact and approximate solutions for $\alpha = \beta = 1$, $q = 0.95$, $k_1 = k_2 = 2$, and $M_1 = M_2 = 4$ in $(x, t) \in [0, 1] \times [0, 1]$ of Example 2.

Algorithm 1 Algorithm for computing the FOFW coefficients and the approximate solution

Step 1: First, construct the fractional-order Fibonacci wavelet (FOFW) basis functions by selecting appropriate values of the resolution level k, the truncation parameter M, and the fractional orders α and β. These basis functions provide a complete and flexible set for approximating the unknown solution over the computational domain.

Step 2: Next, compute the operational matrices (OMs) of integration and variable-order fractional differentiation corresponding to the FOFW basis. These matrices allow the transformation of fractional integro-differential operators into algebraic matrix forms.

Step 3: Based on the structure and order of the given variable-order fractional integro-differential equation (VOFIDE), represent the highest-order derivative of the unknown function using the FOFW expansion introduced in (21).

Step 4: Substitute the obtained FOFW expansions and the corresponding operational matrices into (30) to express all differential and integral terms of the governing equation in terms of known matrices and unknown coefficient vectors.

Step 5: Apply the collocation method by enforcing (30) at selected collocation points in the spatial–temporal domain, which yields a system of algebraic equations.

Step 6: Solve the resulting algebraic system using an appropriate numerical solver to determine the unknown FOFW coefficients associated with the approximate solution.

Step 7: Finally, substitute the computed coefficients into (28) to reconstruct the approximate solution of the original variable-order fractional integro-differential equation.

9 Conclusion

In this study, an efficient numerical scheme based on fractional-order Fibonacci wavelets (FOFWs) has been developed for approximating the solutions of variable-order fractional integro-differential (VOFIDE) equations. The proposed method provides a systematic framework that combines accuracy, computational efficiency, and flexibility in handling variable-order fractional operators.

First, the theoretical foundations of the method were established through several theorems related to the convergence analysis of the FOFW expansion. These results guarantee the reliability of the approximation and confirm that the proposed approach converges to the exact solution under appropriate conditions. Such theoretical validation plays a crucial role in demonstrating the robustness of the method. Next, the construction of the operational matrices (OMs) for variable-order fractional differentiation and integration was presented in detail. By employing these operational matrices, the original VOFIDE equations were successfully transformed into a system of algebraic equations. This transformation significantly reduces the computational complexity of the problem and simplifies the numerical implementation. To verify the effectiveness and accuracy of the proposed approach, several numerical examples were presented. The numerical results illustrated through tables and graphical plots, clearly demonstrate the high accuracy and stability of the method. In particular, the results show that increasing the parameters k and M leads to a noticeable improvement in accuracy, while the computational cost increases in a controlled and predictable manner. This confirms the efficiency of the method and its suitability for practical applications.

In summary, both the theoretical analysis and numerical experiments confirm that the proposed FOFW-based operational matrix method is a reliable and effective tool for solving VOFIDEs. Due to its flexibility and accuracy, the method can be extended to more complex models, including nonlinear variable-order fractional problems and higher-dimensional systems, which represent natural directions for future investigation.

Declarations

Author Contributions

All authors contributed equally to the study design, data analysis, and manuscript preparation, and share equal responsibility for the content of the paper.

Acknowledgments

The authors received no specific funding for this research. They would like to thank all colleagues and reviewers whose constructive comments significantly improved the quality of this manuscript.

Conflict of Interest

The authors declare that they have no conflict of interest.

Artificial Intelligence Statement

Artificial intelligence (AI) tools, including large language models, were used solely for language editing and improving readability. AI tools were not used for generating ideas, performing analyses, interpreting results, or writing the scientific content. All scientific conclusions and intellectual contributions were made exclusively by the authors.

Publisher's Note

The publisher remains neutral with regard to jurisdictional claims in published maps and institutional affiliations.

References

[1] Agrawal, O.P. (2004). "A general formulation and solution scheme for fractional optimal control problems". *Nonlinear Dynamics*, 38, 323–337. DOI: https://doi.org/10.1007/s11071-004-3764-6

[2] Avazzadeh, Z., Beygi Rizi, Z., Maalek Ghaini, F.M., Loghmani, G.B. (2012). "A numerical solution of nonlinear parabolic-type Volterra partial integro-differential equations using radial basis functions". *Engineering Analysis with Boundary Elements*, 36, 881–893. DOI: https://doi.org/10.1016/j.enganabound.2011.09.013

[3] Cao, J., Qiu, Y., Song, G. (2017). "A compact finite difference scheme for variable order subdiffusion equation". *Communications in Nonlinear Science and Numerical Simulation*, 48, 140–149. DOI: https://doi.org/10.1016/j.cnsns.2016.12.022

[4] Ciesielski, M., Leszczynski, J.S. (2006). "Numerical solutions to boundary value problem for anomalous diffusion equation with Riesz–Feller fractional operator". *Journal of Theoretical and Applied Mechanics*, 44(2), 393–403.

[5] Coimbra, C.F.M. (2003). "Mechanics with variable-order differential operators". *Annalen der Physik*, 11–12, 692–703. DOI: https://doi.org/10.1002/andp.200351511-1203

[6] Dabiri, A., Parsa Moghaddam, B., Tenreiro Machado, J.A. (2018). "Optimal variable-order fractional PID controllers for dynamical systems". *Journal of Computational and Applied Mathematics*, 339, 40–48. DOI: https://doi.org/10.1016/j.cam.2018.02.029

[7] Das, Sh. (2008). "Functional fractional calculus for system identification and controls". *Springer, Berlin, Heidelberg*. DOI: https://doi.org/10.1007/978-3-540-72703-3

[8] Das, Sh. (2011). "Functional fractional calculus". *Springer, Berlin, Heidelberg*. DOI: https://doi.org/10.1007/978-3-642-20545-3

[9] Doha, E.H., Abdelkawy, M.A., Amin, A.Z.M., Baleanu, D. (2017). "Spectral technique for solving variable-order fractional Volterra integro-differential equations". *Numerical Methods for Partial Differential Equations*, 34(5), 1659–1677. DOI: https://doi.org/10.1002/num.22233

[10] Duarte, F.B.M., Machado, J.A.T. (2002). "Chaotic phenomena and fractional-order dynamics in the trajectory control of redundant manipulators". *Nonlinear Dynamics*, 29, 342–362. DOI: https://doi.org/10.1023/A:1016559314798

[11] Engheta, N. (1996). "On fractional calculus and fractional multipoles in electromagnetism". *IEEE Transactions on Antennas and Propagation*, 44, 554–566. DOI: https://doi.org/10.1109/8.489308

[12] Falcon, S., Plaza, A. (2007). "The k-Fibonacci sequence and the Pascal 2-triangle". *Chaos, Solitons and Fractals*, 33(1), 38–49. DOI: https://doi.org/10.1016/j.chaos.2006.10.022

[13] Firoozjaee, M.A., Jafari, H., Lia, A., Baleanu, D. (2018). "Numerical approach of Fokker–Planck equation with Caputo–Fabrizio fractional derivative using Ritz approximation". *Journal of Computational and Applied Mathematics*, 339, 367–373. DOI: https://doi.org/10.1016/j.cam.2017.05.022

[14] Gafiychuk, V., Datsko, B., Meleshko, V. (2008). "Mathematical modeling of time fractional reaction–diffusion systems". *Journal of Computational and Applied Mathematics*, 220, 215–225. DOI: https://doi.org/10.1016/j.cam.2007.08.011

[15] Hassani, H., Machado, J.A.T., Avazzadeh, Z., Naraghirad, E. (2020). "Generalized shifted Chebyshev polynomials: Solving a general class of nonlinear variable order fractional PDE". *Communications in Nonlinear Science and Numerical Simulation*, 85, 105229. DOI: https://doi.org/10.1016/j.cnsns.2020.105229

[16] Heydari, M.H., Razzaghi, M., Cattani, C. (2023). "Fractional Chebyshev cardinal wavelets: Application for fractional quadratic integro-differential equations". *International Journal of Computer Mathematics*, 100(3), 479–496. DOI: https://doi.org/10.1080/00207160.2022.2122052

[17] Heydari, M.H. (2018). "A new direct method based on the Chebyshev cardinal functions for variable-order fractional optimal control problems". *Journal of the Franklin Institute*, 355(12), 4970–4995. DOI: https://doi.org/10.1016/j.jfranklin.2018.05.025

[18] Heydari, M.H. (2016). "A new approach of the Chebyshev wavelets for the variable-order time fractional mobile-immobile advection-dispersion model". *arXiv preprint*, arXiv:1605.06332.

[19] Heydari, M.H., Avazzadeh, Z. (2018). "Legendre wavelets optimization method for variable-order fractional Poisson equation". *Chaos, Solitons and Fractals*, 112, 180–190. DOI: https://doi.org/10.1016/j.chaos.2018.04.028

[20] Hosseininia, M., Heydari, M.H., Avazzadeh, Z., Maalek Ghaini, F.M. (2018). "Two-dimensional Legendre wavelets for solving variable-order fractional nonlinear advection–diffusion equation with variable coefficients". *International Journal of Nonlinear Sciences and Numerical Simulation*, 19(7–8), 793–802. DOI: https://doi.org/10.1515/ijnsns-2018-0168

[21] Hosseinzadeh, N., Shivanian, E., Fairooz, M.Z., Chegini, T.G. (2025). "A robust RBF-FD technique combined with polynomial enhancements for valuing European options in jump-diffusion frameworks". *International Journal of Dynamics and Control*, 13, 212. DOI: https://doi.org/10.1007/s40435-025-01722-6

[22] Jiang, W., Liu, N. (2017). "A numerical method for solving the time variable fractional order mobile–immobile advection–dispersion model". *Applied Numerical Mathematics*, 119, 18–32. DOI: https://doi.org/10.1016/j.apnum.2017.03.014

[23] Keshavarz, E., Ordokhani, Y., Razzaghi, M. (2018). "The Taylor wavelets method for solving the initial and boundary value problems of Bratu-type equations". *Applied Numerical Mathematics*, 128, 205–216. DOI: https://doi.org/10.1016/j.apnum.2018.02.001

[24] Kulish, V.V., Lage, J.L. (2002). "Application of fractional calculus to fluid mechanics". *Journal of Fluids Engineering*, 124, 803–806. DOI: https://doi.org/10.1115/1.1478062

[25] Masood, Z., Majeed, K., Samar, R., Raja, M.A.Z. (2017). "Design of Mexican Hat Wavelet neural networks for solving Bratu type nonlinear systems". *Neurocomputing*, 221, 1–14. DOI: https://doi.org/10.1016/j.neucom.2016.08.079

[26] Moghaddam, B.P., Tenreiro Machado, J.A. (2017). "Time analysis of forced variable-order fractional Van der Pol oscillator". *The European Physical Journal Special Topics*, 226(16), 3803–3810. DOI: https://doi.org/10.1140/epjst/e2018-00019-7

[27] Nagy, A.M., Sweilam, N.H. (2018). "Numerical simulations for a variable order fractional cable equation". *Acta Mathematica Scientia*, 38(2), 580–590. DOI: https://doi.org/10.1016/S0252-9602(18)30767-7

[28] Nandal, S., Narain Pandey, D. (2021). "Numerical technique for fractional variable-order differential equation of fourth-order with delay". *Applied Numerical Mathematics*, 161, 391–407. DOI: https://doi.org/10.1016/j.apnum.2020.11.021

[29] Nemati, S., Kalansara, Z.R. (2022). "A low-cost computational method for solving nonlinear fractional delay differential equations". *Communications in Nonlinear Science and Numerical Simulation*, 114, 106650. DOI: https://doi.org/10.1016/j.cnsns.2022.106650

[30] Odibat, Z., Shawagfeh, N.T. (2007). "Generalized Taylor's formula". *Applied Mathematics and Computation*, 186(1), 286–293. DOI: https://doi.org/10.1016/j.amc.2006.07.102

[31] Oldham, K.B. (2010). "Fractional differential equations in electrochemistry". *Advances in Engineering Software*, 41, 9–12. DOI: https://doi.org/10.1016/j.advengsoft.2008.12.012

[32] Rahimkhani, P., Ordokhani, Y. (2021). "Orthonormal Bernoulli wavelets neural network method and its application in astrophysics". *Computational & Applied Mathematics*, 40(3), 78. DOI: https://doi.org/10.1007/s40314-021-01475-w

[33] Rahimkhani, P., Ordokhani, Y. (2021). "Numerical investigation of distributed-order fractional optimal control problems via Bernstein wavelets". *Optimal Control Applications & Methods*, 42(1), 355–373. DOI: https://doi.org/10.1002/oca.2679

[34] Rahimkhani, P., Ordokhani, Y. (2022). "A modified numerical method based on Bernstein wavelets for numerical assessment of fractional variational and optimal control problems". *Iranian Journal of Science and Technology, Transactions of Electrical Engineering*, 46, 1041–1056. DOI: https://doi.org/10.1007/s40998-022-00522-4

[35] Rahimkhani, P., Ordokhani, Y. (2020). "The bivariate Müntz wavelets composite collocation method for solving space-time-fractional partial differential equations". *Computational & Applied Mathematics*, 39, 115. DOI: https://doi.org/10.1007/s40314-020-01141-7

[36] Rahimkhani, P., Ordokhani, Y., Babolian, E. (2018). "Müntz–Legendre wavelet operational matrix of fractional-order integration and its applications for solving the fractional pantograph differential equations". *Numerical Algorithms*, 77, 1283–1305. DOI: https://doi.org/10.1007/s11075-017-0363-4

[37] Rahimkhani, P., Ordokhani, Y., Lima, P.M. (2019). "An improved composite collocation method for distributed-order fractional differential equations based on fractional Chelyshkov wavelets". *Applied Numerical Mathematics*, 145, 1–27. DOI: https://doi.org/10.1016/j.apnum.2019.05.023

[38] Ramirez, L.E.S., Coimbra, C. (2011). "On the variable order dynamics of the nonlinear wake caused by a sedimenting particle". *Physica D*, 240, 1111–1118. DOI: https://doi.org/10.1016/j.physd.2011.04.001

[39] Ramirez, L.E.S., Coimbra, C., Kobayashi, M. (2007). "A variable order constitutive relation for viscoelasticity". *Annalen der Physik*, 16, 543–552. DOI: https://doi.org/10.1002/andp.200751907-803

[40] Sabermahani, S., Ordokhani, Y. (2020). "A new operational matrix of Müntz–Legendre polynomials and Petrov–Galerkin method for solving fractional Volterra–Fredholm integro-differential equations". *Computational Methods for Differential Equations*, 8(3), 408–423. DOI: https://doi.org/10.22034/cmde.2020.32623.1515

[41] Sabermahani, S., Ordokhani, Y. (2020). "Two-dimensional Müntz–Legendre hybrid functions: theory and applications for solving fractional-order partial differential equations". *Computational & Applied Mathematics*, 39(2), 111. DOI: https://doi.org/10.1007/s40314-020-1137-5

[42] Sabermahani, S., Ordokhani, Y., Hassani, H. (2021). "General Lagrange scaling functions: Application in general model of variable order fractional partial differential equations". *Computational & Applied Mathematics*, 40(8), 1–21. DOI: https://doi.org/10.1007/s40314-021-01667-4

[43] Sabermahani, S., Ordokhani, Y., Lima, P.M. (2020). "A novel Lagrange operational matrix and Tau-Collocation method for solving variable-order fractional differential equations". *Iranian Journal of Science and Technology, Transactions A: Science*, 44(1), 127–135. DOI: https://doi.org/10.1007/s40995-019-00797-z

[44] Sabermahani, S., Ordokhani, Y., Rahimkhani, P. (2022). "Application of two-dimensional Fibonacci wavelets in fractional partial differential equations arising in the financial market". *International Journal of Applied and Computational Mathematics*, 8, 129. DOI: https://doi.org/10.1007/s40819-022-01329-x

[45] Sabermahani, S., Ordokhani, Y., Yousefi, S.A. (2020). "Fibonacci wavelets and their applications for solving two classes of time-varying delay problems". *Optimal Control Applications & Methods*, 41(2), 395–416. DOI: https://doi.org/10.1002/oca.2549

[46] Samko, S.G., Ross, B. (1993). "Integration and differentiation to a variable fractional order". *Integral Transforms and Special Functions*, 1(4), 277–300. DOI: https://doi.org/10.1080/10652469308819027

[47] Samko, S.G. (1995). "Fractional integration and differentiation of variable order". *Analysis Mathematica*, 21, 213–236. DOI: https://doi.org/10.1007/BF01911126

[48] Samko, S.G. (2013). “Fractional integration and differentiation of variable order: An overview”. *Nonlinear Dynamics*, 71, 653–662. DOI: https://doi.org/10.1007/s11071-012-0485-0

[49] Shekari, Y., Tayebi, A., Heydari, M.H. (2017). “A meshless method for solving two-dimensional variable-order time fractional advection–diffusion equation”. *Journal of Computational Physics*, 340, 655–669. DOI: https://doi.org/10.1016/j.jcp.2017.03.061

[50] Shivanian, E., Jafarabadi, A., Chegini, T.G., Dinmohammadi, A. (2025). “Analysis of a time-dependent source function for the heat equation with nonlocal boundary conditions through a local meshless procedure”. *Computational & Applied Mathematics*, 44, 282. DOI: https://doi.org/10.1007/s40314-025-03246-3

[51] Soon, C.M., Coimbra, C.F.M., Kobayashi, M.H. (2005). “The variable viscoelasticity oscillator”. *Annalen der Physik*, 14(6), 378–389. DOI: https://doi.org/10.1002/andp.20055170602

[52] Sun, H.G., Chen, Y.Q., Chen, W. (2011). “Random-order fractional differential equation models”. *Signal Processing*, 91, 525–530. DOI: https://doi.org/10.1016/j.sigpro.2010.01.027

[53] Tarasov, V.E. (2010). *Fractional dynamics: Applications of fractional calculus to dynamics of particles, fields and media*. Springer, Berlin, Heidelberg. DOI: https://doi.org/10.1007/978-3-642-14003-7

[54] Wei, S., Chen, W., Zhang, Y., Wei, H., Garrard, R.M. (2018). “A local radial basis function collocation method to solve the variable-order time fractional diffusion equation in a two-dimensional irregular domain”. *Numerical Methods for Partial Differential Equations*, 34(4), 1209–1223. DOI: https://doi.org/10.1002/num.22253

[55] Xu, Y., He, Z. (2013). “Existence and uniqueness results for Cauchy problem of variable-order fractional differential equations”. *Journal of Applied Mathematics and Computation*, 43(1–2), 295–306. DOI: https://doi.org/10.1007/s12190-013-0664-2

[56] Zahra, W.K., Hikal, M.M. (2015). “Non standard finite difference method for solving variable order fractional optimal control problems”. *Journal of Vibration and Control*, 23(6), 948–958. DOI: https://doi.org/10.1177/1077546315586646

[57] Zhou, F., Xu, X. (2019). “Numerical solution of fractional Volterra–Fredholm integrodifferential equations with mixed boundary conditions via Chebyshev wavelet method”. *International Journal of Computer Mathematics*, 96(2), 436–456. DOI: https://doi.org/10.1080/00207160.2018.1521517

Authors Bio-sketches

Shiva Karimi is currently a PhD candidate in numerical analysis in the Department of Applied Mathematics at Imam Khomeini International University, Qazvin, Iran. She received her B.Sc. and M.Sc. degrees in applied mathematics from Imam Khomeini International University.

Elyas Shivanian is a professor of applied mathematics at Imam Khomeini International University. Corresponding author: Email: shivanian@sci.ikiu.ac.ir

Zahra Barikbin is an assistant professor of applied mathematics at Imam Khomeini International University.